Deep learning in magnetic resonance prostate segmentation: A review and a new perspective

David Gillespie[a,1], Connah Kendrick[a], Ian Boon[b], Cheng Boon[c], Tim Rattay[d], Moi Hoon Yap[a,*]

[a]*Manchester Metropolitan University, John Dalton Building, Chester Street, Manchester M1 5GD, UK*
[b]*NHS, The Leeds Teaching Hospital, Great George St, Leeds, LS1 3EX, UK*
[c]*NHS, The Clatterbridge Cancer Center, Lower Lane, Liverpool L9 7AL, UK*
[d]*Leicester University,Leicester Cancer Research Centre, University Road, Leicester, LE1 7RH, UK*

ABSTRACT

Prostate radiotherapy is a well established curative oncology modality, which in future will use Magnetic Resonance Imaging (MRI)-based radiotherapy for daily adaptive radiotherapy target definition. However the time needed to delineate the prostate from MRI data accurately is a time consuming process. Deep learning has been identified as a potential new technology for the delivery of precision radiotherapy in prostate cancer, where accurate prostate segmentation helps in cancer detection and therapy. However, the trained models can be limited in their application to clinical setting due to different acquisition protocols, limited publicly available datasets, where the size of the datasets are relatively small. Therefore, to explore the field of prostate segmentation and to discover a generalisable solution, we review the state-of-the-art deep learning algorithms in MR prostate segmentation; provide insights to the field by discussing their limitations and strengths; and propose an optimised 2D U-Net for MR prostate segmentation. We evaluate the performance on four publicly available datasets using Dice Similarity Coefficient (DSC) as performance metric. Our experiments include within dataset evaluation and cross-dataset evaluation. The best result is achieved by composite evaluation (DSC of 0.9427 on Decathlon test set) and the poorest result is achieved by cross-dataset evaluation (DSC of 0.5892, Prostate X training set, Promise 12 testing set). We outline the challenges and provide recommendations for future work. Our research provides a new perspective to MR prostate segmentation and more importantly, we provide standardised experiment settings for researchers to evaluate their algorithms. Our code is available at https://github.com/AIEMMU/MRI_Prostate.

1. Introduction

Following an initial diagnosis of cancer, many patients are referred to specialist centres for radiotherapy. Radiotherapy is an important part of the potentially curative treatment of both breast and prostate cancer, where it is used in 4 out of 10 of all cancer curative treatment modalities Cullen et al. (2019). The number of radiotherapy courses in Europe was estimated at 1.7M in 2012. The largest number of radiotherapy courses was for breast cancers (396,891) and second largest was for prostate cancer (243,669) (Borras et al., 2016). The projected incidence of cancer continues to rise with prostate cancer being the most commonly diagnosed cancer in the United Kingdom

Prostate Cancer (2020). The evidence for both curative Dearnaley et al. (2016) and palliative radiotherapy in prostate cancer is well established Parker et al. (2018).

The future of prostate radiotherapy will be the development of MR-only based radiotherapy Pathmanathan et al. (2018). In MRI-only prostate radiotherapy pathway, the significant benefit would be MRI allows better soft tissue definition, which means precision radiotherapy can be further improved. Precision radiotherapy allows potentially increased in cure rates and further avoidance of normal tissue toxicities Pathmanathan et al. (2018). Prostate cancer patients have a high cure rate, and therefore, any reduction of long term side effect would be advantageous. The challenge of MR-only radiotherapy is it requires daily adaptive radiotherapy contouring for delivery. herefore this paper will only address the use of MRI data for delineating the prostate volume.

*Corresponding author: Tel.: +44 161 247 1503;
e-mail: M.Yap@mmu.ac.uk (Moi Hoon Yap)

At present, clinical oncologists manually contour or delineate the primary cancer volume as part of the target volume definition process of the radiotherapy workflow. In contouring prostate cancer in the curative setting, firstly clinicians will delineate the primary cancer target volume. This will be the primary prostate volume, and in high risks, prostate cancer clinicians may potentially include seminal vesicles structures and suspected nodal volumes. Next, clinicians will outline adjacent Organ At Risks (OARs) including the rectum, bowels, bladder, and femoral heads which are the normal structures to avoid radiotherapy doses. However, this contouring process has been identified as the weakest link with wide-ranging variation amongst clinicians Vinod et al. (2016). This is where auto-segmentation using deep learning algorithms can be helpful.

Artificial Intelligence (AI) has been identified by the UK NHS and the Royal College of Radiologists as a major technological advancement to radiology and oncology Topol (2019), for the use of deep learning image segmentation. Image segmentation is the process of segmenting an image into various classes based on their pixel values. It is widely used in various fields such as autonomous driving, visual tracking, but it is still one of the most challenging aspects of analysing medical images. The task of segmenting organs or lesions from the background of CT or MRI has improved recently with the development of Convolutional Neural Networks (CNNs) and the use of Fully Convolution Networks (FCNs) Long et al. (2015). The introduction of the U-Net Ronneberger et al. (2015), Residual Convolution Blocks Alom et al. (2018) and attention mechanisms Oktay et al. (2018) has significantly improved performance and detections over earlier systems based on edge detection algorithms. The promising nature of deep learning segmentation approaches has put them as a primary option and solution for health care professionals.

However, while literature discusses the potentials of deep learning image segmentation approaches, there are few reviews on the pitfalls of architectures or the discussion regarding data acquisition. While new models can achieve state-of-the-art benchmarks on publicly available datasets, these scores are rarely reflected when used on real-world data acquired from clinical institutions. The lack of large prostate segmentation datasets, or reproducible results lead to the state-of-the-art segmentation models failing to generalise to real-world scenarios.

The aim of this paper was to review state-of-the-art models used in prostate MRI segmentation, to discuss their limitations and strengths, and to conduct a study comparing performance of an optimised 2D U-Net to segment the prostate in four publicly available prostate MRI datasets. We also discuss the potential of creating a protocol for the evaluation and testing of future algorithms, to allow for reproducibility and to be explored by our fellow peers.

2. Review on Existing Methods

Early attempts to automate the process of delineating the prostate relied on edge or region based models, which incorporated prior knowledge or used atlas-based segmentation Sharp et al. (2014); Iglesias and Sabuncu (2015); Klein et al. (2008). They use an approach that matches manually selected regions on a target image to selected reference images, where the ground truth reference segmentation mask is mapped back to the target image. However, these approaches are heavily reliant on the atlas selection strategy as well as how well the region was selected Schipaanboord et al. (2019); Peressutti et al. (2016). To improve upon atlas-based approaches, deep learning methods have been applied to medical imaging segmentation tasks resulting in significant improvements, especially with the recent developments of CNNs, FCNs Long et al. (2015) and the U-Net Ronneberger et al. (2015). Deep learning approaches can learn a rich set of features to perform pixel-wise image segmentation or classification Ronneberger et al. (2015); Guo et al. (2015) offering a computation advantage over atlas-based methods, as they can inference directly on new data.

A CNN is a neural network that learns by feeding input into a network, that consists of layers (convolutions, maxpools, relu), where the output from one layer is fed into the next layer. Through this process, the network learns to recognise patterns, and abstractions to be able to classify input data correctly Long et al. (2015); Bibault et al. (2016). The use of CNNs has achieved outstanding results for automatically detecting prostate cancer in multi panoramic MRI Yang et al. (2017); Wang et al. (2018), as well as patch-based ensembling methods for patch-based segmentation Jia et al. (2018).

A FCN Long et al. (2015) is similar to a CNN, however, it does not contain any dense layers that are common in CNN, and the last layer is replaced with a simple convolutional layer with a stride of 1 and a kernel size of 1. This allows the network to output a feature map that, contains pixel-wise predictions for each class from the full image. Ronneberger et al. Ronneberger et al. (2015) expanded upon the FCN with the development of the U-Net. It uses a CNN as a downward sampling path, with an up-sampling operation, increasing the resolution of the output feature maps. It also uses skip connections, to provide more information to the feature maps that are placed within the up-sampling operations Ronneberger et al. (2015). The U-Net is one of the most popular networks for image segmentation on medical images Zhou et al. (2018); Çiçek et al. (2016); Alom et al. (2018); Isensee et al. (2018); Oktay et al. (2018); Dong et al. (2017); Ibtehaz and Rahman (2020); Alom et al. (2019).

Clark et al. Clark et al. (2017a,b) was one of the first to deploy a U-Net to delineate the prostate. They use a trained standard VGG network Simonyan and Zisserman (2014), to detect slices in Diffusion-Weighted MRI (DWI) that contained a part of the prostate. They then used a U-Net to segment the whole prostate gland and transitional zone, before using a U-Net to segment the Prostate. Using this simple approach, they were able to achieve a DSC of 0.93 for the prostate on an in house dataset. However, when they validated on T2-weighted (T2W) MRI data from the Promise 12 challenge Litjens et al. (2014), they were only able to achieve a DSC of 0.86. Zhu et al. Zhu et al. (2017) proposed a deeply supervised U-Net architecture for prostate segmentation. It utilises residual blocks to reduce the number of parameters compared to the original U-Net Zhu et al. (2017) and uses a deep supervision strategy. The deep supervision strategy is to supervise the hidden layers within the

network and propagate it to the lower levels of the network. Using more than one supervision within the network leads to enhancing the feature maps of the network, thus better segmentation Zhu et al. (2019b). Zhu et al. Zhu et al. (2017) were able to out perform the original U-Net to segment the prostate, and scored a dice coefficient score of 0.885 on their own internal dataset.

Tian et al. Tian et al. (2018) developed the PSNET from the FCN Long et al. (2015). The network was fine-tuned on an in-house dataset consisting of 42 T2W MRI volumes and using patients from two open-source prostate segmentation datasets, the PROMISE12 challenge Litjens et al. (2014) and the ISBI2013 Bloch et al. (2015) dataset. Using a five-fold cross-validation procedure using 112 out of 140 volumes for training, they achieved a validation DSC of 0.85. Karimi et al. Karimi et al. (2018) followed a similar approach, they used a smaller FCN consisting of 3 layers, and used a much smaller dataset consisting of 49 T2W axial MRI images and with 26 MRI images from the PROMISE12 challenge Litjens et al. (2014) using patients that did not have an endorectal coil. Using a cross-validation scheme, Karimi et al. Karimi et al. (2018) was able to achieve a 0.88 DSC on their validation set. Both networks were able to achieve high DSCs on their respective validation datasets, demonstrating the potential of deep learning for MRI prostate image segmentation.

The U-Net architecture has since been adapted to be able to segment prostates from 3D MRI volumes instead of MRI slices by Milletari et al. Milletari et al. (2016). They trained their network on the Promise12 challenge dataset Litjens et al. (2014), where they show their network performed significantly better than other networks at the time. They also proposed a loss function based on the Dice coefficient. The use of this loss function and data augmentation allowed Milletari et al. Milletari et al. (2016) to achieve an even higher DSC than their implementation trained using a multi logistic loss function Milletari et al. (2016). Yu et al. Yu et al. (2017) improved upon this, by adding residual connections to the network into the 3D segmentation network, which helped to improve the prostate segmentation. It also used a sum operation instead of the concatenation operation features into the up-sampling layer, turning it into a ResNet-U-Net hybrid.

To improve upon the accuracy of prostate segmentation, Zhu et al. Zhu et al. (2019b) proposed the use of a cascaded U-Net. Where the output from the first network, segmented the whole prostate gland, and the segmented gland was fed into the second network to segment the peripheral zone. Using this method, they were able to achieve a mean DSC of 0.92 for segmenting the whole prostate, and 79.7 for the peripheral zone on their own dataset. Using a similar strategy as Zhu et al. Zhu et al. (2017), Wang et al. Wang et al. (2019) proposed a deep supervision strategy for a 3D U-Net and group dilated convolutions for segmentation of the prostate gland. The deep learning strategy was proposed to prevent exploding or vanishing gradients when training deep models, but also to force the hidden layers to favour highly discriminate features. Wang et al. Wang et al. (2019) also used group dilated convolutions to extract more global contextual information, as they increase the

receptive field of the network, without adding extra parameters and memory cost to the network. They also used a combined loss function consisting of cross-entropy loss and cosine, which measures the similarity and dissimilarity between segmentation and manual contours. These techniques improved the segmentation accuracy of their network, achieving a DSC of 0.86 on their internal dataset, and a score of 0.88 on the Promise-12 challenge dataset Litjens et al. (2014).

Liu et al. Liu et al. (2019b) proposed a network to segment the prostate zones using FCN with a feature pyramid attention mechanism. They used a ResNet50 as the backbone of their network, with a feature pyramid network to capture features at multiple scales, and a simple decoder. The feature pyramid attention can capture strong semantic information at multiple scales, which are combined to generate a high-resolution feature representation. This helps to improve the segmentation results of Lui et al. Liu et al. (2019b), over the original U-Net Ronneberger et al. (2015), where it achieved a DSC of 0.74 and 0.86 on the prostatic transitional zone and peripheral zone from 63 patients from the Promise 12 dataset Litjens et al. (2014). They were able also to achieve a DSC of 0.74 and 0.79 of the prostatic transitional zone and peripheral zone on an external dataset.

Zabihollahya et al. Zabihollahy et al. (2019) proposed a U-Net network architecture that would segment the prostate zones on T2W and apparent diffusion coefficient (ADC) map prostate MRI images separately. They trained 2 networks per modality, one to segment the whole prostate gland and another to segment the central gland. They then use a post-processing process to create the contours of the whole prostate, central gland and the peripheral zone on both of the modalities Zabihollahy et al. (2019). Using this methodology, they were able to achieve on their own internal dataset a mean DSC of 0.92, 0.91 and 86.22 for the whole gland, central gland and peripheral zone respectively on the T2W MRI images. They were also able to achieve similar scores on the apparent diffusion coefficient MRI images with 0.89, 0.86 and 0.83 for the whole gland, central gland and peripheral zone Zabihollahy et al. (2019).

Nie and Shen Nie and Shen (2019) proposed a semantic guided strategy to learn discriminative features, to improve delineation of the prostate. They also proposed a soft contour constraint mechanism to model the blurry boundary detections, to improve the segmentation of the prostate. They trained their network on 50 prostate cancer patients, with ground truths annotated manually of the rectum, prostate and bladder. Using a 5 k-fold validation scheme, they obtained a DSC of 0.975, 0.932, and 0.918 for the bladder, prostate and rectum respectively. Their approach outperformed state of the art techniques Nie and Shen (2019) achieved a DSC of 0.92 on the Promise12 dataset Litjens et al. (2014) and a score of 0.89 on the hidden test set of the Promise12 challenge. Zhu et al. Zhu et al. (2019a) proposed a boundary-weighted segmentation loss, to increase the sensitivity of the network to boundary segmentation. They also introduced a boundary weighted transfer learning approach was exploited to overcome the challenge of small datasets that are available for training. Using this approach, and leveraging several datasets, they were able to achieve the state of the art

results on the Promise12 Challenge test dataset Litjens et al. (2014), achieving a score of 0.8958.

2.1. Generalisation

For prostate delineating, MRI scans normally have a third dimension. This third dimension allows for valuable information to be extracted from the Z axis, which makes a 3D U-Net the most appropriate choice Isensee et al. (2018). However, this limits training data, and uses alot more memory for computation versus a 2D U-net. Isensee et al. (2018) proposed a novel approach, that condenses domain knowledge, and chooses the best nnU-Net configuration (2D or 3D) for a given dataset. This approach has managed to achieve state of the art results in 19 competitions at the time of its release Isensee et al. (2019). They trained a 2D and a 3D variant nnU-net with a 5 fold cross-validation scheme, with no manual intervention for both the Promise12 challenge Litjens et al. (2014) and the Medical Decathlon dataset Simpson et al. (2019). Using an ensembling approach with the output from their 3D and 2D nnU-Net, they managed to achieve a DSC of 0.8965 on the Promise12 Challenge Litjens et al. (2014) and a 0.77 and 0.90 DSC for the peripheral zone and transitional zone on the Decathlon dataset Simpson et al. (2019). In their paper, they also demonstrate that common modifications to U-Nets to improve segmentation results, do not always necessarily result in a good performance or are superior to a properly tuned baseline method Isensee et al. (2019).

One of the main limitations of the above papers is their focus on single site prostate MRI vendors for network training to improve their performance. This allows for the model to perform well on their own data, but it does not take into consideration how it may perform on data from another site, or MRI vendor. This is a large issue for prostate segmentation, as there are differences between MRI scanner vendors and protocols Rundo et al. (2019); Zavala-Romero et al. (2020); Liu et al. (2020). Rundo et al. Rundo et al. (2019) attempted to solve this issue by using a channel-wise feature recalibration to improve the segmentation results. They also incorporate squeeze and excitation blocks into their network Rundo et al. (2019). They compared their network against U-Net Ronneberger et al. (2015), Pix to Pix Isola et al. (2017), MS-D net and a continuous max flow model Qiu et al. (2014). They performed well when their network was trained on all of the dataset's, but less so when trained only on one or two of the datasets Rundo et al. (2019). However, their network was still robust, and their DSC score were very similar to the other networks it tested against.

Another attempt to generalise to multi-site MRI images was performed by Zavala Romero et al. Zavala-Romero et al. (2020) who implemented a 3D multi-stream U-Net, and proposed data prepossessing, that would normalise the data between MRI vendors. Six models were trained (two for each vendor, and two with combined vendor data) and their data was analysed, revealing that the combined vendor models, performed better than their singular data model for detecting the peripheral zone with a DSC of 0.81. However, it performed worse than the singular data models for detecting the whole prostate. This seems to be in line with the literature, where mixing datasets, can lead to poorer performance, than a model trained on a singular dataset Zech et al. (2018); Onofrey et al. (2019). Liu et al. Liu et al. (2020), also worked on the problem of generalisation of segmentation models, implementing a Multi-site network that focused on learning the universal representation across the datasets and MRI scanners. They also developed a technique called Domain-Specific Batch normalisation, that was able to estimate the statistics and perform normalisation for each site the network had been trained on, helping to strengthen the segmentation.

3. Datasets

The application of deep learning to the delineation of the prostate has achieved greater accuracy and results than previous manual or atlas-based methods Onofrey et al. (2019). To achieve this, networks are typically trained on large datasets that are annotated for a certain task such as imagenet Deng et al. (2009). However, to gather such a large dataset for medical imaging is fraught with challenges.

Even though terabytes of data is being created within the NHS, and is stored on secure local servers, there are governance issues, that restrict the sharing of this data between health centres and deep learning practitioners. The medical data, must be stored locally and only be accessed on site. This could be negated through the use of decentralised federated learning Shi et al. (2019), where the model moves where it is training and the data stays at the local site. Which allows for privacy and security concerns to be addressed regarding. However, the infrastructure and logistics are currently not in place to allow this to be explored yet in practice Onofrey et al. (2019). Though this data may be available, it may not be labeled, or annotated in a way to allow it to be used with deep learning. To curate and collect medical imaging datasets, can be laborious, tedious and expensive to annotate new images. Thus it is important to explore current datasets and exploit them to create a generalisable network for delineating the prostate (Onofrey et al., 2019).

3.1. Limited Availability of Medical Imaging

Within the United Kingdom, the National Health Service maintains the Diagnostic Imaging Dataset (DID) which has detailed information of diagnostics imaging performed but does not retain the actual medical images. Diagnostic Imaging Dataset (DID) NHS (2020) From April 2019 to April 2020, a total of 42,330,840 imaging were performed. There is very limited publicly available imaging dataset in the United Kingdom. Only 3 large databases were identified as follow:

- **UK Biobank**. Largest UK biobank established for long-term follow up on 500,000 healthy volunteer. Dataset of abdominal, brain and heart MRI. Suitable for AI training and access on application.

- **REQUITE collaboration**. Largest comprehensive radiotherapy database on breast (n=2069), prostate (n=1808) and lung (n=561) cancer. Radiotherapy dataset includes radiotherapy images DICOMs (n=17,107) and DVHs (n=12684). Data on patient toxicities are also available.

Excellent radiotherapy database for AI training with access on applicationSeibold et al. (2019).

- **National COVID-19 Chest Image Database (NCCID)**. Newly formed national database to collect X-ray, CT and MRI of COVID-19 patients. Data collection phase. Aimed for development and validation for AI machine learning. Data access on application.

Limited good quality radiology and oncology imaging are available for artificial intelligence which will likely continue to be a barrier for artificial intelligence development for healthcare within the UK NICE (2018). For the purpose of the segmentation of the prostate for this paper, we worked with 4 publicly available datasets. These included:

- **The Promise 12 dataset Litjens et al. (2014)**. Which consists of 50 patients T2 MRI scans of the prostate region. The data is this dataset, is representative of a clinical setting, and has been acquired from multiple centres, that use a variety of vendors and acquisition protocols. A Radiographist resident or image analysis researcher, created the contours for segmentation, with a resident radiographer with 6 years of MRI prostate experience checked and corrected the contours.

- **Prostate X Litjens et al. (2017)**. The largest dataset of prostate data contains 300 patients data, in either T3 or T2 MRI scans. 98 T2 weighted MRI scans have been annotated by a a medical student and then corrected by a urologist expert Meyer et al. (2019).

- **NCI-ISBI 2013 Challenge Bloch et al. (2015)**. This dataset contains 60 patient Dicom files, of 1.5 MRI scans and T3 MRI SCANS. These were acquired from Radboud University Nijmegen Medical Centre [RUNMC],Netherland. The contours created for segmentation were either created by Drs. Nicolas Bloch (Boston University School of Medicine) and Mirabela Rusu (Case Western University) or Drs. Henkjan Huisman, Geert Litjens, or Futterer at RUNMC

- **The Decathlon Medical dataset Simpson et al. (2019)**. The decathlon dataset consists of 32 multi-modal MRI scans of the prostate, which has been acquired from RUNMC. The data was donated by Drs Geert Litjens and Bram van Ginneken from RUNMC.

As summarised in Table 1, a majority of previous research used private databases for their experiments, which makes it difficult to reproduce their work. This makes it difficult to ascertain if the modifications they have mentioned contributes to increase in their various metric scores or if the model is well tuned Isensee et al. (2019).

The delineation of the prostate is a labour-intensive process performed manually by a trained clinician but is essential for radiotherapy. This is a time-consuming process, and the delineated prostate annotation can be subject to a variety of bias Roques (2014); Njeh (2008); Ghose et al. (2012), but an accurate delineation is critical when planning treatments for patients.

4. Comparative Study

As part of this review, we implement a 2D U-Net architecture using the Ranger optimiser Wright (2019) and Mish Activation Misra (2020), to segment the prostate from MRI data. The ranger optimiser is a combination of two optimisers, Rectified Adam Liu et al. (2019a) and Lookahead Zhang et al. (2019) optimisers. These were inspired by recent work, in understanding the loss surfaces, and how initial training can have a large impact on the convergence of networks Liu et al. (2019a). LookAhead keeps two sets of weights, and interpolates between them during training, it allows one set of faster weights to explore the loss landscape to choose an optimum path, where the slower weights stay behind to provide long term stability Liu et al. (2019a). In the case of the Ranger optimiser, the faster weights use the Rectified Adam weights (Wright, 2019). Mish is a new activation function that can be displayed mathematically as

$$x = xtanh(softplus(x)) \tag{1}$$

It is a self regularising non-monotonic activation function, which has improved the performance of other networks, just by changing the activation functions within these networks to Mish Wright (2019).

We evaluate the ability of these slight changes to the U-Net configuration and its effect on performances on four publicly available datasets, i.e. the Promise 12 Litjens et al. (2014), Prostate X Litjens et al. (2017), NIC ISBI 2013 Bloch et al. (2015) and the Decathlon Medical Dataset Simpson et al. (2019). We evaluate models trained on each dataset and a combination of all, on a test set with DSC. The goal of this approach is to segue to a generalisable segmentation approach, that is both repeatable, open and usable by clinicians and oncologists. All of the images were pre-processed with an adaptive histogram and normalized during training. All of our code is available at https://github.com/AIEMMU/MRI_Prostate.

4.1. Training

For training, each model was trained with the ranger optimiser, with a learning rate of 1e-3 and a weight decay of 0.01, and using a flat + cosine anneal training curve with PyTorch. Each model is trained for 20 epochs, then fine-tuned and trained for a further 20 epochs with a batch size of 8 at a resolution of 448px x 448px. The loss function for the model is a combination of Dice Loss Milletari et al. (2016), focal loss Lin et al. (2017) and cross-entropy.

For each model, the data was split at a random 80:20 split for training and testing. For validation, the training data was also a random 80:20 split. To avoid the model overfitting, data augmentation was used to to create new versions of the same image. Zhang et al. (2016).The augmentations using during training the neural network, included rotation, translation and vertical or horizontal flips Dong et al. (2017). Additional augmentations were added to change the image quality using different contrast, lighting and adding noise.

The training was performed on a desktop computer with a 24GB RTX Titan, i5-9600K CPU, 32GB of RAM and a 2TB SSD drive. Training time for each model took on average 40

Table 1. Summary of different methods and datasets pertaining to MRI prostate segmentation. DSC–Dice Similarity Coefficient, FPR–False Positive Rate, FNR–False Negative Rate, HD–Hausdorff Distance, AVD–Absolute Volume Distance, ABD–Absolute Boundary Distance, ASD–Average Surface Distance, RVD–Relative Volume Difference, aRVD–absolute Relative Volume Difference, MSD–Mean and Standard Deviation, AAD–Average Absolute Distance, MAD–Maximum Absolute Distance

Publication	Datasets	Metrics	Modality	Loss Functions
Tian et al. (2018)	41 patient in house dataset Promise12 Litjens et al. (2014) ISBI2013 Bloch et al. (2015)	DSC, RVD, HD, ASD	T2W MRI	Weighted Cross Entropy
Clark et al. (2017a)	104 in house dataset Promise12 (Litjens et al., 2014)	DSC Sensitivity Specificity Accuracy	mpMRI T2W MRI	Dice loss
Karimi et al. (2018)	49 patient in house dataset 26 training images Promise12 Litjens et al. (2014)	DSC	T2W MRI	Squared Euclidean distance with elastic-net regularization
Zhu et al. (2017)	81 patient in house dataset	DSC	3T MRI	Dice Loss
Milletari et al. (2016)	Promise12 Litjens et al. (2014)	DSC, HD	T2 MRI	Dice Loss
Zhu et al. (2019b)	163 patients in house dataset	DSC, FPR, FNR	DWI, T2W MRI	Dice loss
Yu et al. (2017)	Promise12 Litjens et al. (2014)	DSC, aRVD, ABD, HD	T2W MRI	Weighted Cross Entropy Loss%
Wang et al. (2019)	40 in house patients Promise12 Litjens et al. (2014)	DSC, HD, aRVD, MSD	T2W MRI	Cosine Similarity and Cross Entropy
Liu et al. (2019b)	319 patients from Prostate X Litjens et al. (2017) 46 patients in house dataset	DSC	3T MRI	Cross Entropy
Zabihollahy et al. (2019)	225 patients in house dataset	DSC, AVD, Precision, Recall, Accuracy	3T MRI	Dice Loss
Nie and Shen (2019)	50 patients in house dataset Promise12Litjens et al. (2014)	DSC, ASD	T2W MRI	Soft Cross Entropy
Zhu et al. (2019a)	Promise12 Litjens et al. (2014) Phillips 3T MRI datasetRundo et al. (2017) Brigham and Women's Hospital Multiparametric MRI Fedorov et al. (2018)	DSC, HD, ABD, RVD	T2W MRI, 3T MRI, mpMRI	Boundary weighted Loss function
Isensee et al. (2019)	Decathlon Prostate Dataset Simpson et al. (2019) Promise12 Litjens et al. (2014)	DSC	T2W MRI	Dice and Cross entropy loss
Rundo et al. (2019)	Philips DatasetRundo et al. (2017) I2CVBLemaître et al. (2015) ISBI2013Bloch et al. (2015)	DSC, Sensitivity, Specificity, SPC, AAD, MAD	T2W MRI	Dice Loss
Zavala-Romero et al. (2020)	550 patient in house dataset	DSC	T2W	Dice Loss
Liu et al. (2020)	ISBI 2013Bloch et al. (2015) I2CVBLemaître et al. (2015)	DSC,AVD	3T MRI, T2W MRI	Dice Loss

minutes, with overall time taking close to 6 hours for all 5 models.

4.2. Results

Table 2. The performance of the optimised 2D U-Net for MRI prostate segmentation on four datasets using Dice Similarity Coefficient (DSC).

		Training Datasets			
	Dataset	Promise 12	Prostate X	Decathlon	NIC ISBI
Testing Datasets	Promise12	*0.9069*	0.8869	0.9239	0.828
	Prostate X	0.5891	*0.9054*	0.9107	0.8011
	Decathlon	0.6055	0.6479	*0.9148*	0.7395
	NIC ISBI	0.6931	0.7463	0.7628	*0.8909*
	Combined	**0.9171**	**0.9061**	**0.9427**	**0.8960**

Table 2 shows the obtained DSC scores on separate test sets for each dataset. We observe that the model that was trained with all of the data outperformed all other models with higher DSC scores. However, we also observe that each of the networks performed well on the decathlon dataset apart from the NIC ISBI trained model. This could be due to a number of reasons. We show similar results to Zavala-Romero et al. (2020), that combining multiple datasets, resulted in an increase in DSC scores.

Figure 1 presents the qualitative results of the segmentation, where the images are from separate Datasets. From left to right, the images are from: Promise12, ProstateX, NIC ISBI and decathlon. Thus, highlighting the capabilities of the network.

5. Challenges, Recommendations and Future Research Direction

This section addresses the challenges of deep learning in MRI prostate segmentation. We provide some recommendations for future research direction and draw a new perspective for this research domain.

5.1. Limited Annotated Data

This paper has presented challenges that still need to be met within the field of segmentation of the prostate from MRI data. This includes the use of private data and a lack of publicly annotated datasets. As many papers within this study, use a private in house dataset, it is not possible to compare fairly against other networks and know what changes to a network impact the performance of a network as discussed in Isensee et al. (2019). Deep learning greatly improves their accuracy by being trained on large datasets within their domain. However, this is a difficult task within the medical imaging, especially with restrictions on patients data and the laborious task of collecting and annotating new images. This restricts the use of AI within a clinical setting. Although, it allows for researchers to innovate and explore new techniques to exploit the small datasets that are available using techniques.

One of such is Mixup a newer data augmentation technique Zhang et al. (2017), which has improved results dramatically

for small datasets, and for models that are not pretrained on similar data. Mixup is a simple concept, which combines two images via an alpha overlay. It has been shown to improve the generalisation of knee segmentation Panfilov et al. (2019) for MRI data. This technique has been expanded to combine latent feature from the layers of a network Verma et al. (2019).

Another approach is using self-supervised learning, where the model can learn representations of the data without using annotated data. This can be accomplished by training the model on tasks such as recognising color spaces Goyal et al. (2019), inpainting Pathak et al. (2016) or predicting image rotations. The learned features using self-supervised tasks are good alternatives for tasks with little data. Goyal et al. Goyal et al. (2019), who via scaling the amount of data available for training, model parameters and hardness of the self-learning task, showed that they equal too or surpassed supervised learning tasks.

5.2. Work Flows

Deep learning attempts to replicate the ground truth labels for segmentation, but variation between clinicians is recognised as one of the weakest link in the contouring process among cancer clinicians Vinod et al. (2016). Clinicians do adopt a QA and peer review to reduce inter-observer variation Huo et al. (2017). However, many clinicians rely on their own experiences and data to outline their own ground truths, which a deep learning model will not have access to. Thus it is important to rethink how segmentation models may be deployed in a clinical setting. Will they be replacing the annotation stage or offer a suggested contour that the clinician may use/edit or allow the clinician to create their annotation.

5.3. Performance Metrics

The training of auto segmenting models via deep learning relies on metrics such as the DSC, HD, or class accuracy. However, these metrics are not sensitive to significant clinical errors. While DSC scores how similar images are, it is insensitive to small changes in border outlines, these small changes may have a significant impact on the deliberating effects for patients. Small offsets, may require new contours to be annotated completely, reducing any time that the deep learning system may have saved. Surface Dice has shown promise as a metric for measuring the performance of an auto segmenting model Nikolov et al. (2018). Yet, Nikolov et al. (2018) to be able to use this metric, they had to employ 3 oncologists to annotate data, and measure an acceptable tolerance for differing organs. This limits the use of this metric, outside head and neck radiography. More metrics need to be explored, that can generalise well to differing organs, and be clinically acceptable as well. Future work will focus on this.

Additionally, apart from using a standard performance metrics, for fair comparison, we recommend to establish standardised experiment protocols where the researchers can compare their algorithms on a standard dataset from multiple vendors. With standardisation of training set and testing set, the protocols can be used to focus solely on the design of the network and augmentation strategies. For reproducibility and transparency of the implementation, the participants would share their codes

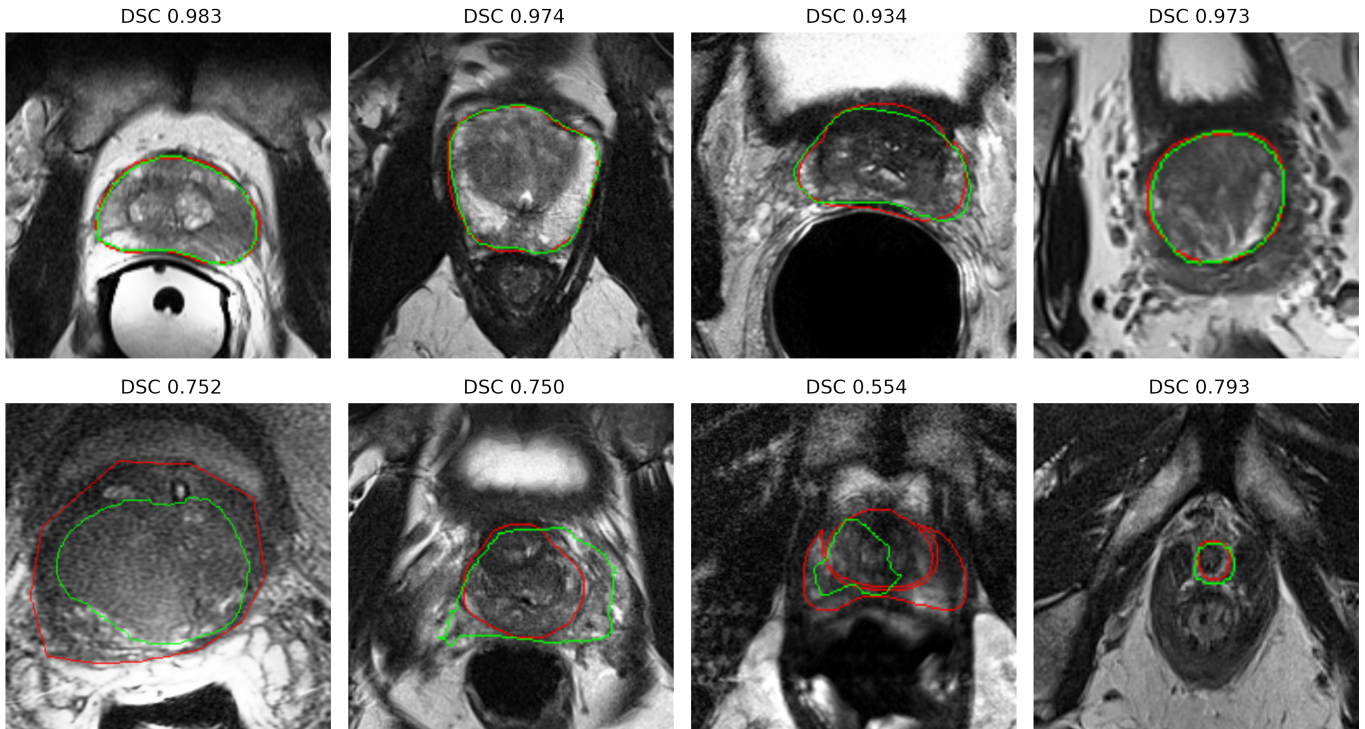| DSC 0.983 | DSC 0.974 | DSC 0.934 | DSC 0.973 |
| DSC 0.752 | DSC 0.750 | DSC 0.554 | DSC 0.793 |

Fig. 1. Examples of the auto prostate delineation, where green is the predicted outline and the red is the ground truth. The top row, are successes with DSC over 0.9. The bottom row are some challenging cases with poorer results. The images from left to right are from the Promise12 dataset, ProstateX dataset, NIC ISBI, Decathlon.

with full details of implementation, as in Fastai and our proposed method here as exemplar.

6. Conclusion

In this paper, we have discussed state-of-the-art deep learning algorithms for MRI prostate segmentation. We have shown the challenges in conducting a fair comparison on the performance of these networks, as most are not reproducible due to their use of in-house datasets. We have demonstrated that an optimised 2D U-Net using existing activation function and optimisers, can achieve high DSC scores on 4 different test datasets. We have also demonstrated that networks trained on the Promise12 Litjens et al. (2014) and ProstateX Litjens et al. (2017) achieved high DSC scores on the Decathlon dataset Simpson et al. (2019) and generalise well to the other datasets. Finally, we address the limitations of MRI prostate segmentation and provide a new perspective. Future work will investigate metrics that can assess a models performance more in line with oncologists expertise.

Acknowledgments

References

Alom, M.Z., Hasan, M., Yakopcic, C., Taha, T.M., Asari, V.K., 2018. Recurrent residual convolutional neural network based on u-net (r2u-net) for medical image segmentation. arXiv preprint arXiv:1802.06955 .

Alom, M.Z., Yakopcic, C., Hasan, M., Taha, T.M., Asari, V.K., 2019. Recurrent residual u-net for medical image segmentation. Journal of Medical Imaging 6, 014006.

Bibault, J.E., Giraud, P., Burgun, A., 2016. Big data and machine learning in radiation oncology: state of the art and future prospects. Cancer letters 382, 110–117.

Bloch, N., Madabhushi, A., Huisman, H., Freymann, J., Kirby, J., Grauer, M., Enquobahrie, A., Jaffe, C., Clarke, L., Farahani, K., 2015. Nci-isbi 2013 challenge: automated segmentation of prostate structures. The Cancer Imaging Archive 370.

Borras, J.M., Lievens, Y., Barton, M., Corral, J., Ferlay, J., Bray, F., Grau, C., 2016. How many new cancer patients in europe will require radiotherapy by 2025? an estro-hero analysis. Radiotherapy and Oncology 119, 5–11.

Çiçek, Ö., Abdulkadir, A., Lienkamp, S.S., Brox, T., Ronneberger, O., 2016. 3d u-net: learning dense volumetric segmentation from sparse annotation, in: International conference on medical image computing and computer-assisted intervention, Springer. pp. 424–432.

Clark, T., Wong, A., Haider, M.A., Khalvati, F., 2017a. Fully deep convolutional neural networks for segmentation of the prostate gland in diffusion-weighted mr images, in: International Conference Image Analysis and Recognition, Springer. pp. 97–104.

Clark, T., Zhang, J., Baig, S., Wong, A., Haider, M.A., Khalvati, F., 2017b. Fully automated segmentation of prostate whole gland and transition zone in diffusion-weighted mri using convolutional neural networks. Journal of Medical Imaging 4, 041307.

Cullen, J., Drabble, D., Castellanos, C., Brissett, L., 2019. Recommendations for achieving a world-class radiotherapy service in the uk. The Tavistock Institute .

Dearnaley, D., Syndikus, I., Mossop, H., Khoo, V., Birtle, A., Bloomfield, D., Graham, J., Kirkbride, P., Logue, J., Malik, Z., et al., 2016. Conventional versus hypofractionated high-dose intensity-modulated radiotherapy for prostate cancer: 5-year outcomes of the randomised, non-inferiority, phase 3 chhip trial. The Lancet Oncology 17, 1047–1060.

Deng, J., Dong, W., Socher, R., Li, L.J., Li, K., Fei-Fei, L., 2009. Imagenet: A large-scale hierarchical image database, in: 2009 IEEE conference on computer vision and pattern recognition, Ieee. pp. 248–255.

Dong, H., Yang, G., Liu, F., Mo, Y., Guo, Y., 2017. Automatic brain tumor de-

tection and segmentation using u-net based fully convolutional networks, in: annual conference on medical image understanding and analysis, Springer. pp. 506–517.

Fastai, . fastai/imagenette. URL: https://github.com/fastai/imagenette.

Fedorov, A., Schwier, M., Clunie, D., Herz, C., Pieper, S., Kikinis, R., Tempany, C., Fennessy, F., 2018. An annotated test-retest collection of prostate multiparametric mri. Scientific data 5, 1–13.

Ghose, S., Oliver, A., Martí, R., Lladó, X., Vilanova, J.C., Freixenet, J., Mitra, J., Sidibé, D., Meriaudeau, F., 2012. A survey of prostate segmentation methodologies in ultrasound, magnetic resonance and computed tomography images. Computer methods and programs in biomedicine 108, 262–287.

Goyal, P., Mahajan, D., Gupta, A., Misra, I., 2019. Scaling and benchmarking self-supervised visual representation learning, in: Proceedings of the IEEE International Conference on Computer Vision, pp. 6391–6400.

Guo, Y., Gao, Y., Shen, D., 2015. Deformable mr prostate segmentation via deep feature learning and sparse patch matching. IEEE transactions on medical imaging 35, 1077–1089.

Huo, M., Gorayski, P., Poulsen, M., Thompson, K., Pinkham, M., 2017. Evidence-based peer review for radiation therapy–updated review of the literature with a focus on tumour subsite and treatment modality. Clinical Oncology 29, 680–688.

Ibtehaz, N., Rahman, M.S., 2020. Multiresunet: Rethinking the u-net architecture for multimodal biomedical image segmentation. Neural Networks 121, 74–87.

Iglesias, J.E., Sabuncu, M.R., 2015. Multi-atlas segmentation of biomedical images: a survey. Medical image analysis 24, 205–219.

Isensee, F., Jäger, P.F., Kohl, S.A., Petersen, J., Maier-Hein, K.H., 2019. Automated design of deep learning methods for biomedical image segmentation. arXiv preprint arXiv:1904.08128 .

Isensee, F., Petersen, J., Klein, A., Zimmerer, D., Jaeger, P.F., Kohl, S., Wasserthal, J., Koehler, G., Norajitra, T., Wirkert, S., et al., 2018. nnunet: Self-adapting framework for u-net-based medical image segmentation. arXiv preprint arXiv:1809.10486 .

Isola, P., Zhu, J.Y., Zhou, T., Efros, A.A., 2017. Image-to-image translation with conditional adversarial networks, in: Proceedings of the IEEE conference on computer vision and pattern recognition, pp. 1125–1134.

Jia, H., Xia, Y., Song, Y., Cai, W., Fulham, M., Feng, D.D., 2018. Atlas registration and ensemble deep convolutional neural network-based prostate segmentation using magnetic resonance imaging. Neurocomputing 275, 1358–1369.

Karimi, D., Samei, G., Kesch, C., Nir, G., Salcudean, S.E., 2018. Prostate segmentation in mri using a convolutional neural network architecture and training strategy based on statistical shape models. International journal of computer assisted radiology and surgery 13, 1211–1219.

Klein, S., Van Der Heide, U.A., Lips, I.M., Van Vulpen, M., Staring, M., Pluim, J.P., 2008. Automatic segmentation of the prostate in 3d mr images by atlas matching using localized mutual information. Medical physics 35, 1407–1417.

Lemaître, G., Martí, R., Freixenet, J., Vilanova, J.C., Walker, P.M., Meriaudeau, F., 2015. Computer-aided detection and diagnosis for prostate cancer based on mono and multi-parametric mri: a review. Computers in biology and medicine 60, 8–31.

Lin, T.Y., Goyal, P., Girshick, R., He, K., Dollár, P., 2017. Focal loss for dense object detection, in: Proceedings of the IEEE international conference on computer vision, pp. 2980–2988.

Litjens, G., Debats, O., Barentsz, J., Karssemeijer, N., Huisman, H., 2017. Prostatex challenge data. The Cancer Imaging Archive 10, K9TCIA.

Litjens, G., Toth, R., van de Ven, W., Hoeks, C., Kerkstra, S., van Ginneken, B., Vincent, G., Guillard, G., Birbeck, N., Zhang, J., et al., 2014. Evaluation of prostate segmentation algorithms for mri: the promise12 challenge. Medical image analysis 18, 359–373.

Liu, L., Jiang, H., He, P., Chen, W., Liu, X., Gao, J., Han, J., 2019a. On the variance of the adaptive learning rate and beyond. arXiv preprint arXiv:1908.03265 .

Liu, Q., Dou, Q., Yu, L., Heng, P.A., 2020. Ms-net: Multi-site network for improving prostate segmentation with heterogeneous mri data. IEEE Transactions on Medical Imaging .

Liu, Y., Yang, G., Mirak, S.A., Hosseiny, M., Azadikhah, A., Zhong, X., Reiter, R.E., Lee, Y., Raman, S.S., Sung, K., 2019b. Automatic prostate zonal segmentation using fully convolutional network with feature pyramid attention. IEEE Access 7, 163626–163632.

Long, J., Shelhamer, E., Darrell, T., 2015. Fully convolutional networks for semantic segmentation, in: Proceedings of the IEEE conference on computer vision and pattern recognition, pp. 3431–3440.

Meyer, A., Rakr, M., Schindele, D., Blaschke, S., Schostak, M., Fedorov, A., Hansen, C., 2019. Towards patient-individual pi-rads v2 sector map: Cnn for automatic segmentation of prostatic zones from t2-weighted mri, in: 2019 IEEE 16th International Symposium on Biomedical Imaging (ISBI 2019), IEEE. pp. 696–700.

Milletari, F., Navab, N., Ahmadi, S.A., 2016. V-net: Fully convolutional neural networks for volumetric medical image segmentation, in: 2016 fourth international conference on 3D vision (3DV), IEEE. pp. 565–571.

Misra, D., 2020. Mish: A self regularized non-monotonic activation function. arXiv preprint arXiv:1908.08681 , 1–14.

NHS, 2020. Diagnostic imaging dataset. URL: https://www.england.nhs.uk/statistics/statistical-work-areas/diagnostic-imaging-dataset.

NICE, 2018. Imaging repositories: Identifying challenges and solutions for the coordinated collection, storage and use of images in cancer research.

Nie, D., Shen, D., 2019. Semantic-guided encoder feature learning for blurry boundary delineation. arXiv preprint arXiv:1906.04306 .

Nikolov, S., Blackwell, S., Mendes, R., De Fauw, J., Meyer, C., Hughes, C., Askham, H., Romera-Paredes, B., Karthikesalingam, A., Chu, C., et al., 2018. Deep learning to achieve clinically applicable segmentation of head and neck anatomy for radiotherapy. arXiv preprint arXiv:1809.04430 .

Njeh, C., 2008. Tumor delineation: The weakest link in the search for accuracy in radiotherapy. Journal of medical physics/Association of Medical Physicists of India 33, 136.

Oktay, O., Schlemper, J., Folgoc, L.L., Lee, M., Heinrich, M., Misawa, K., Mori, K., McDonagh, S., Hammerla, N.Y., Kainz, B., et al., 2018. Attention u-net: Learning where to look for the pancreas. arXiv preprint arXiv:1804.03999 .

Onofrey, J.A., Casetti-Dinescu, D.I., Lauritzen, A.D., Sarkar, S., Venkataraman, R., Fan, R.E., Sonn, G.A., Sprenkle, P.C., Staib, L.H., Papademetris, X., 2019. Generalizable multi-site training and testing of deep neural networks using image normalization, in: 2019 IEEE 16th International Symposium on Biomedical Imaging (ISBI 2019), IEEE. pp. 348–351.

Panfilov, E., Tiulpin, A., Klein, S., Nieminen, M.T., Saarakkala, S., 2019. Improving robustness of deep learning based knee mri segmentation: Mixup and adversarial domain adaptation, in: Proceedings of the IEEE International Conference on Computer Vision Workshops, pp. 0–0.

Parker, C.C., James, N.D., Brawley, C.D., Clarke, N.W., Hoyle, A.P., Ali, A., Ritchie, A.W., Attard, G., Chowdhury, S., Cross, W., et al., 2018. Radiotherapy to the primary tumour for newly diagnosed, metastatic prostate cancer (stampede): a randomised controlled phase 3 trial. The Lancet 392, 2353–2366.

Pathak, D., Krahenbuhl, P., Donahue, J., Darrell, T., Efros, A.A., 2016. Context encoders: Feature learning by inpainting, in: Proceedings of the IEEE conference on computer vision and pattern recognition, pp. 2536–2544.

Pathmanathan, A.U., van As, N.J., Kerkmeijer, L.G., Christodouleas, J., Lawton, C.A., Vesprini, D., van der Heide, U.A., Frank, S.J., Nill, S., Oelfke, U., et al., 2018. Magnetic resonance imaging-guided adaptive radiation therapy: a "game changer" for prostate treatment? International Journal of Radiation Oncology* Biology* Physics 100, 361–373.

Peressutti, D., Schipaanboord, B., van Soest, J., Lustberg, T., van Elmpt, W., Kadir, T., Dekker, A., Gooding, M., 2016. Tu-ab-202-10: How effective are current atlas selection methods for atlas-based auto-contouring in radiotherapy planning? Medical physics 43, 3738–3739.

Prostate Cancer, U., 2020. Prostate cancer becomes most commonly diagnosed cancer in uk, but research is at a standstill. URL: https://prostatecanceruk.org/about-us/news-and-views/2020/6/most-common-cancer-in-uk.

Qiu, W., Yuan, J., Ukwatta, E., Sun, Y., Rajchl, M., Fenster, A., 2014. Dual optimization based prostate zonal segmentation in 3d mr images. Medical image analysis 18, 660–673.

Ronneberger, O., Fischer, P., Brox, T., 2015. U-net: Convolutional networks for biomedical image segmentation, in: International Conference on Medical image computing and computer-assisted intervention, Springer. pp. 234–241.

Roques, T., 2014. Patient selection and radiotherapy volume definition—can we improve the weakest links in the treatment chain? Clinical oncology 26, 353–355.

Rundo, L., Han, C., Nagano, Y., Zhang, J., Hataya, R., Militello, C., Tangher-

loni, A., Nobile, M.S., Ferretti, C., Besozzi, D., et al., 2019. Use-net: Incorporating squeeze-and-excitation blocks into u-net for prostate zonal segmentation of multi-institutional mri datasets. Neurocomputing 365, 31–43.

Rundo, L., Militello, C., Russo, G., Garufi, A., Vitabile, S., Gilardi, M.C., Mauri, G., 2017. Automated prostate gland segmentation based on an unsupervised fuzzy c-means clustering technique using multispectral t1w and t2w mr imaging. Information 8, 49.

Schipaanboord, B., Boukerroui, D., Peressutti, D., Van Soest, J., Lustberg, T., Dekker, A., van Elmpt, W., Gooding, M.J., 2019. An evaluation of atlas selection methods for atlas-based automatic segmentation in radiotherapy treatment planning. IEEE transactions on medical imaging 38, 2654–2664.

Seibold, P., Webb, A., Aguado-Barrera, M.E., Azria, D., Bourgier, C., Brengues, M., Briers, E., Bultijnck, R., Calvo-Crespo, P., Carballo, A., et al., 2019. Requite: a prospective multicentre cohort study of patients undergoing radiotherapy for breast, lung or prostate cancer. Radiotherapy and Oncology 138, 59–67.

Sharp, G., Fritscher, K.D., Pekar, V., Peroni, M., Shusharina, N., Veeraraghavan, H., Yang, J., 2014. Vision 20/20: perspectives on automated image segmentation for radiotherapy. Medical physics 41.

Shi, Z., Zhovannik, I., Traverso, A., Dankers, F.J., Deist, T.M., Kalendralis, P., Monshouwer, R., Bussink, J., Fijten, R., Aerts, H.J., et al., 2019. Distributed radiomics as a signature validation study using the personal health train infrastructure. Scientific data 6, 1–8.

Simonyan, K., Zisserman, A., 2014. Very deep convolutional networks for large-scale image recognition. arXiv preprint arXiv:1409.1556 .

Simpson, A.L., Antonelli, M., Bakas, S., Bilello, M., Farahani, K., Van Ginneken, B., Kopp-Schneider, A., Landman, B.A., Litjens, G., Menze, B., et al., 2019. A large annotated medical image dataset for the development and evaluation of segmentation algorithms. arXiv preprint arXiv:1902.09063 .

Tian, Z., Liu, L., Zhang, Z., Fei, B., 2018. Psnet: prostate segmentation on mri based on a convolutional neural network. Journal of Medical Imaging 5, 021208.

Topol, E., 2019. The topol review. Preparing the Healthcare Workforce to Deliver the Digital Future , 1–48.

Verma, V., Lamb, A., Beckham, C., Najafi, A., Mitliagkas, I., Lopez-Paz, D., Bengio, Y., 2019. Manifold mixup: Better representations by interpolating hidden states, in: International Conference on Machine Learning, pp. 6438–6447.

Vinod, S.K., Jameson, M.G., Min, M., Holloway, L.C., 2016. Uncertainties in volume delineation in radiation oncology: a systematic review and recommendations for future studies. Radiotherapy and Oncology 121, 169–179.

Wang, B., Lei, Y., Tian, S., Wang, T., Liu, Y., Patel, P., Jani, A.B., Mao, H., Curran, W.J., Liu, T., et al., 2019. Deeply supervised 3d fully convolutional networks with group dilated convolution for automatic mri prostate segmentation. Medical physics 46, 1707–1718.

Wang, Z., Liu, C., Cheng, D., Wang, L., Yang, X., Cheng, K.T., 2018. Automated detection of clinically significant prostate cancer in mp-mri images based on an end-to-end deep neural network. IEEE transactions on medical imaging 37, 1127–1139.

Wright, L., 2019. Ranger deep learning optimizer. URL: `https://github.com/lessw2020/Ranger-Deep-Learning-Optimizer`.

Yang, X., Liu, C., Wang, Z., Yang, J., Le Min, H., Wang, L., Cheng, K.T.T., 2017. Co-trained convolutional neural networks for automated detection of prostate cancer in multi-parametric mri. Medical image analysis 42, 212–227.

Yu, L., Yang, X., Chen, H., Qin, J., Heng, P.A., 2017. Volumetric convnets with mixed residual connections for automated prostate segmentation from 3d mr images, in: Thirty-first AAAI conference on artificial intelligence, pp. 0–1.

Zabihollahy, F., Schieda, N., Krishna Jeyaraj, S., Ukwatta, E., 2019. Automated segmentation of prostate zonal anatomy on t2-weighted (t2w) and apparent diffusion coefficient (adc) map mr images using u-nets. Medical physics 46, 3078–3090.

Zavala-Romero, O., Breto, A.L., Xu, I.R., Chang, Y.C.C., Gautney, N., Pra, A.D., Abramowitz, M.C., Pollack, A., Stoyanova, R., 2020. Segmentation of prostate and prostate zones using deep learning: A multi-mri vendor analysis. Strahlentherapie und Onkologie , 1–11.

Zech, J.R., Badgeley, M.A., Liu, M., Costa, A.B., Titano, J.J., Oermann, E.K., 2018. Variable generalization performance of a deep learning model to detect pneumonia in chest radiographs: a cross-sectional study. PLoS medicine 15, e1002683.

Zhang, C., Bengio, S., Hardt, M., Recht, B., Vinyals, O., 2016. Understanding deep learning requires rethinking generalization. arXiv preprint arXiv:1611.03530 .

Zhang, H., Cisse, M., Dauphin, Y.N., Lopez-Paz, D., 2017. mixup: Beyond empirical risk minimization. arXiv preprint arXiv:1710.09412 .

Zhang, M., Lucas, J., Ba, J., Hinton, G.E., 2019. Lookahead optimizer: k steps forward, 1 step back, in: Advances in Neural Information Processing Systems, pp. 9597–9608.

Zhou, Z., Siddiquee, M.M.R., Tajbakhsh, N., Liang, J., 2018. Unet++: A nested u-net architecture for medical image segmentation, in: Deep Learning in Medical Image Analysis and Multimodal Learning for Clinical Decision Support. Springer, pp. 3–11.

Zhu, Q., Du, B., Turkbey, B., Choyke, P.L., Yan, P., 2017. Deeply-supervised cnn for prostate segmentation, in: 2017 International Joint Conference on Neural Networks (Ijcnn), IEEE. pp. 178–184.

Zhu, Q., Du, B., Yan, P., 2019a. Boundary-weighted domain adaptive neural network for prostate mr image segmentation. IEEE transactions on medical imaging 39, 753–763.

Zhu, Y., Wei, R., Gao, G., Ding, L., Zhang, X., Wang, X., Zhang, J., 2019b. Fully automatic segmentation on prostate mr images based on cascaded fully convolution network. Journal of Magnetic Resonance Imaging 49, 1149–1156.

Supplementary Material

The codebase for this paper, experiments and processing code is available at https://github.com/AIEMMU/MRI_Prostate